Cell Research (2015) 25:851-863.

www.nature.com/cr

ORIGINAL ARTICLE

Generation of fertile offspring from *Kit*^{w}/*Kit*^{wv} mice through differentiation of gene corrected nuclear transfer embryonic stem cells

Yan Yuan[1, *], Quan Zhou[1, *], Haifeng Wan[2, *], Bin Shen[1, *], Xuepeng Wang[2, 3], Mei Wang[2, 4], Chunjing Feng[2, 3], Mingming Xie[2, 5], Tiantian Gu[2], Tao Zhou[1], Rui Fu[2], Xingxu Huang[6], Qi Zhou[2], Jiahao Sha[1], Xiao-Yang Zhao[2]

[1]State Key Laboratory of Reproductive Medicine, Department of Histology and Embryology, Nanjing Medical University, Nanjing, Jiangsu 210029, China; [2]State Key Laboratory of Reproductive Biology, Institute of Zoology, Chinese Academy of Sciences, Beijing 100101, China; [3]Graduate School of Chinese Academy of Sciences, Beijing 100049, China; [4]College of Life Sciences, Hunan Normal University, Changsha, Hunan 410081, China; [5]College of Life Science, Anhui University of China, Hefei, Anhui 230601, China; [6]MOE Key Laboratory of Model Animal for Disease Study, Model Animal Research Center of Nanjing University, Nanjing Biomedical Research Institute, National Resource Center for Mutant Mice, Nanjing, Jiangsu 210061, China

Genetic mutations could cause sperm deficiency, leading to male infertility. Without functional gametes in the testes, patients cannot produce progeny even with assisted reproduction technologies such as *in vitro* fertilization. It has been a major challenge to restore the fertility of gamete-deficient patients due to genetic mutations. In this study, using a *Kit*^{w}/*Kit*^{wv} mouse model, we investigated the feasibility of generating functional sperms from gamete-deficient mice by combining the reprogramming and gene correcting technologies. We derived embryonic stem cells from cloned embryos (ntESCs) that were created by nuclear transfer of *Kit*^{w}/*Kit*^{wv} somatic cells. Then we generated gene-corrected ntESCs using TALEN-mediated gene editing. The repaired ntESCs could further differentiate into primordial germ cell-like cells (PGCLCs) *in vitro*. RFP-labeled PGCLCs from the repaired ntESCs could produce functional sperms in mouse testes. In addition, by co-transplantation with EGFP-labeled testis somatic cells into the testes where spermatogenesis has been chemically damaged or by transplantation into *Kit*^{w}/*Kit*^{wv} infertile testes, non-labeled PGCLCs could also produce haploid gametes, supporting full-term mouse development. Our study explores a new path to rescue male infertility caused by genetic mutations.

***Keywords*:** male infertility; reprogramming; gene correction; germ cell specification; *Kit* mutation.
Cell Research (2015) **25**:851-863. doi:10.1038/cr.2015.74; published online 19 June 2015

Introduction

Male infertility accounts for about half of human infertility [1]. Many male infertility patients carry genetic defects [2], including deletion of the azoospermia factor c region on Y chromosome [3], small deletions or insertions and single-base mutations in *androgen receptor* (*AR*), *deleted in azoospermia-like* (*DAZL*) [4], and *CAG* triplet repeat expansion in *AR* [5]. It is difficult for gamete-deficient patients with genetic mutations to produce offspring by assisted reproductive technologies [6]. In addition, genetic mutations from the father can be transmitted to offspring [7]. Cell therapies are one of the most promising strategies to rescue this type of infertility.

c-Kit is a highly conserved gene among mammalian species and plays important roles in male germ cell development [8]. When *c-Kit* is dysfunctional, the spermatogonial cells cannot enter meiosis, resulting in azoospermia in mice [9]. There are several natural azoospermia mouse models with *c-Kit* gene mutations [8].

*These four authors contributed equally to this work.
Correspon dence: Qi Zhou[a], Jiahao Sha[b], Xiao-Yang Zhao[c]
[a]Tel: +86-10-6480 -7299; Fax: +86-10-6480-7299
E-mail: qzhou@ioz.ac.cn
[b]Tel: +86-25-8686-2908; Fax: +86-25-8686-2908
E-mail: shajh@njmu@edu.cn
[c]Tel: +86-10-8261-9843; Fax: +86-10-8261-9843
E-mail: xyzhao@ioz.ac.cn
Received 2 December 2014; revised 29 March 2015; accepted 26 April 2015; published online 19 June 2015

Among these variable mutations, *W* and *WV* mutations are located in the trans-membrane domain and the kinase domain of the c-Kit protein, respectively [10]. These two functional domains are conserved between mouse and human. Only double heterozygous mutations lead to infertility, while heterozygosity of *W* or *WV* mutation alone does not cause infertility. Mutant mice carrying biallelic heterozygous mutations mimic the phenotype of male infertility in human, thereby serving as an excellent animal model to develop therapeutic strategies.

Somatic cell reprogramming is a promising way to regenerate pluripotent stem cells (PSCs) from differentiated cells [11]. The two major approaches, somatic cell nuclear transfer (SCNT) and reprogramming of somatic cells into induced PSCs (iPSCs), have been successfully applied to mouse and human cells [12-15]. There have been reports on successful rescue of disease phenotypes in some mouse models, such as mice carrying mutations in *Crygc* [16], *Lrrk2* [17], and *Bcl11a* [18], by combing somatic cell reprogramming and gene correction technologies. However, whether this approach can be used to rescue male infertility remains unclear. Moreover, it has yet to be determined whether gene-corrected cells maintain their genome integrity after serial processes of reprogramming and gene correction.

In this study, we first isolated the tail tip fibroblasts (TTFs) from adult Kit^{w}/Kit^{wv} mutant mice and then derived embryonic stem cells (ESCs) from these cloned blastocysts obtained by SCNT (the produced ESCs were called Kit^{w}/Kit^{wv} ntESCs). The *W* mutation of the Kit^{w}/Kit^{wv} ntESC was corrected without introducing any exogenous DNA. The corrected ntESCs were further differentiated into primordial germ cell-like cells (PGCLCs) and then transplanted into mouse testes for spermatogenesis re-establishment. Our study provides a therapeutic strategy for the regenerative medicine of male infertility.

Results

Derivation of ntESCs from Kit^{w}/Kit^{wv} mouse fibroblasts

TTFs were isolated from the Kit^{w}/Kit^{wv} male mouse and used as donor cells, while B6D2F1 M II oocytes were used as the recipients for nuclear transfer (Figure 1A and 1B). In total, 30 reconstructed embryos were activated and developed into blastocysts (Figure 1C). Six blastocysts were plated in the four-well plate pre-coated with feeder cells and cultured with N2B27 medium supplemented with leukemia inhibitory factor (LIF) and 2i (PD0325901 and CHIR99021). Three outgrowths appeared 4 days later. After splitting and replating in a four-well plate, two stable embryonic stem cell lines (named W-1 and W-2, respectively) were obtained (Figure 1D). Karyotype analysis revealed that these two cell lines had normal karyotypes (Figure 1E). Immunofluorescence results showed that both cell lines expressed pluripotency markers Oct4, Nanog, and SSEA1 (Figure 1F). Real-time PCR results showed that the embryoid bodies derived from the *in vitro* differentiation of W-1 cells expressed typical markers of all three germ layers (Supplementary information, Figure S1). Furthermore, "all-ES" mice were produced by tetraploid complementation with W-1 cells (Figure 1G), which inherited the somatic *W* and *WV* mutations (Figure 1H). In summary, the ntESCs derived from nuclear transfer embryos are authentic PSCs.

W point-mutation correction and germ cell specification of repaired ntESCs in vivo

To generate germ cells from the Kit^{w}/Kit^{wv} ntESCs, we performed gene correction in these ntESCs and induced them to undergo *in vitro* differentiation (Figure 2A). To improve the efficiency of mutation correction through homologous recombination, we designed TALEN to generate DNA double-stranded break specifically at the *W* mutation locus (Figure 2B). The donor vector was constructed by inserting the 5′ and 3′ homology arms and a piggyBac-NEO cassette (sitting between these two arms) into a vector containing the HSV-TK negative selection cassette. The TALEN expression vector and the donor vector were electroporated into the W-1 cells. Neomycin (G418) and ganciclovir (GANC) double-resistant colonies were obtained 7 days later (Figure 2C and 2D). Clones with the correct genomic modification were identified by PCR and Southern blot analyses using primers and probes lying outside of the homology arms (Figure 2E and 2F). To remove the piggyBac selection cassette from these correctly targeted clones, we transfected the piggyBac transponsase and then derived clonal lines, which were then screened by PCR genotyping and sequencing. As expected, sequence analysis confirmed that the *W* mutation was not found in either allele, and that the transposon excision yielded a *TTAA* sequence (replacing the original *CTCA* sequence), which did not change any amino acids of the c-Kit protein (Figure 2G). The repaired cell lines also had a normal karyotype (Supplementary information, Figure S2A), and could differentiate into embryoid bodies with the expression of all three germ layer markers (Supplementary information, Figure S2B). Western blot showed that there was no significant difference in the expression level of the c-Kit protein among the three cell lines (W-1, W-1R and WV-1 (a Kit^{WV}/Kit^{+} ESC line); Supplementary information, Figure S2C). The top 20 potential off-target sites of TALEN cleavage were surveyed by PCR analysis and sequencing, and no mutation was identified in any of the clones

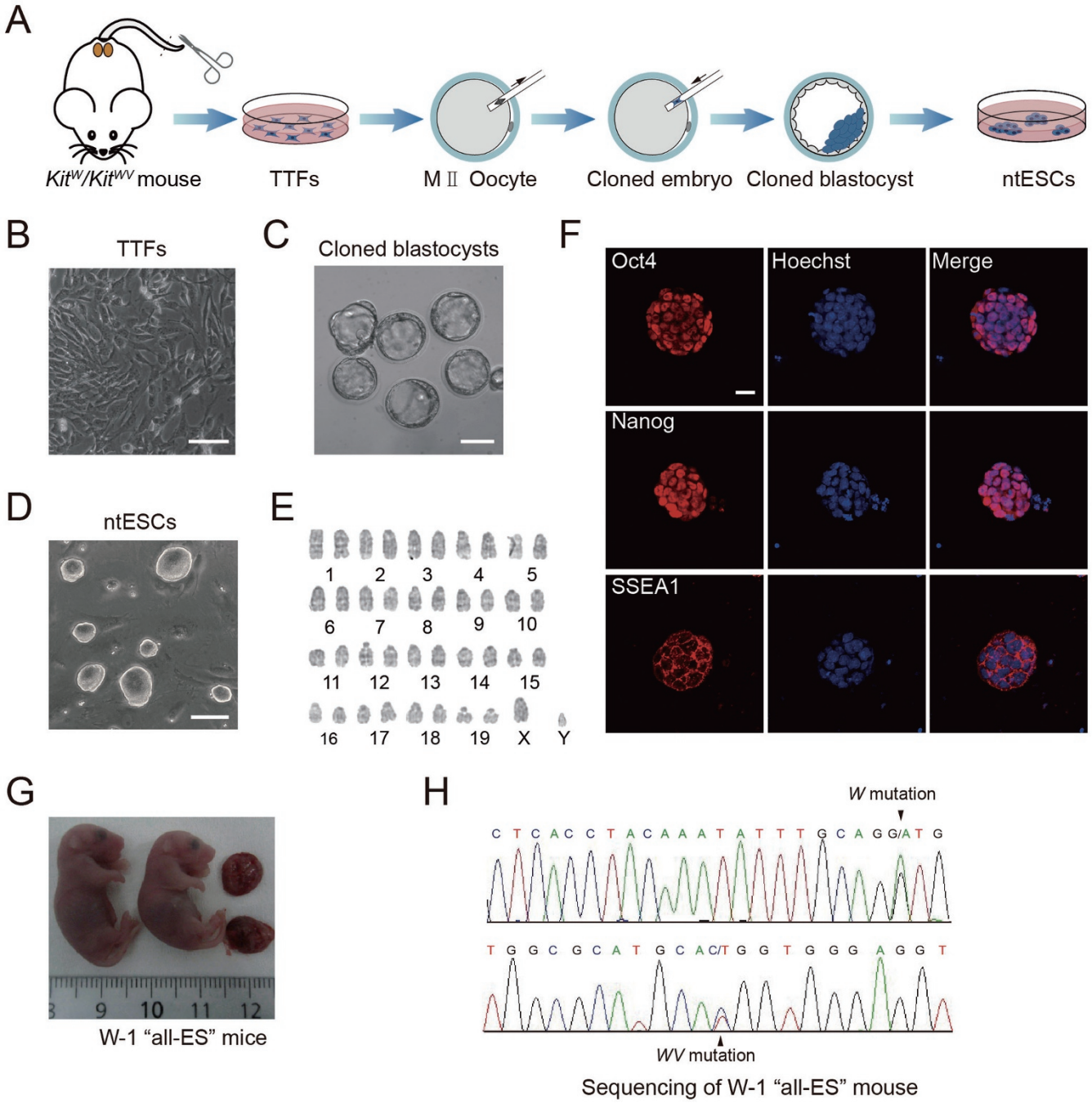

Figure 1 The pluripotency of *Kit*^{W}/*Kit*^{WV} ntESCs (related to Supplementary information, Figure S1 and Table S3). **(A)** Scheme for derivation of ntESCs from SCNT embryos. **(B)** Image of TTFs obtained from the *Kit*^{W}/*Kit*^{WV} adult mouse. Scale bar = 100 μm. **(C)** The TTF nuclear-transferred blastocysts. Scale bar = 100 μm. **(D)** Morphology of W-1 embryonic stem cell line. Scale bar = 100 μm. **(E)** Karyotype of the W-1 embryonic stem cell line. **(F)** Immunostaining of W-1 ESCs (Oct4, Nanog, and SSEA1). Nuclei were stained with Hoechst 33342 (blue). Scale bar = 50 μm. **(G)** W-1 ESCs produced "all-ES" mouse by tetraploid complementation. **(H)** DNA sequencing of the *W* and *WV* point mutation loci in the W-1 "all-ES" mouse.

(Supplementary information, Table S1).

c-Kit gene is critical for the germ cell specification [19, 20]. To validate the function of the corrected *c-Kit* gene, we first examined the *in vivo* germ cell specification of W-1 cells and the repaired ntESCs (W-1R and W-2R) in tetraploid complementation embryos. Following the in-

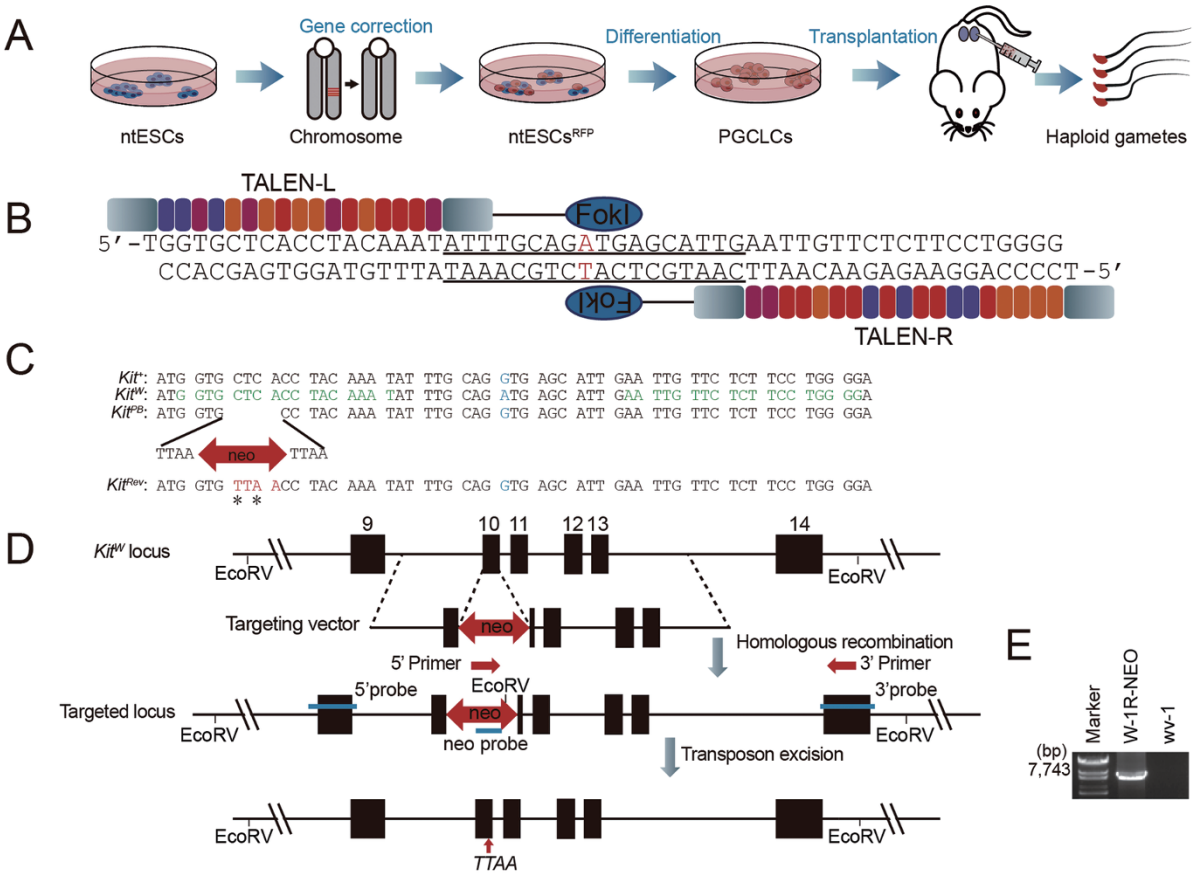
A
Gene correction
Differentiation
Transplantation
ntESCs
Chromosome
ntESCs^RFP
PGCLCs
Haploid gametes
B
TALEN-L
FokI
5′-TGGTGCTCACCTACAAATATTTGCAGATGAGCATTGAATTGTTCTCTTCCTGGGG
CCACGAGTGGATGTTTATAAACGTCTACTCGTAACTTAACAAGAGAAGGACCCCT-5′
FokI
TALEN-R
C
Kit+: ATG GTG CTC ACC TAC AAA TAT TTG CAG GTG AGC ATT GAA TTG TTC TCT TCC TGG GGA
KitW: ATG GTG CTC ACC TAC AAA TAT TTG CAG ATG AGC ATT GAA TTG TTC TCT TCC TGG GGA
KitPB: ATG GTG CC TAC AAA TAT TTG CAG GTG AGC ATT GAA TTG TTC TCT TCC TGG GGA
TTAA neo TTAA
KitRev: ATG GTG TTA ACC TAC AAA TAT TTG CAG GTG AGC ATT GAA TTG TTC TCT TCC TGG GGA
D
KitW locus
EcoRV
9
10 11
12 13
14
Targeting vector
neo
Homologous recombination
5′ Primer
3′ Primer
Targeted locus
5′probe
3′probe
neo probe
Transposon excision
TTAA
E
Marker
W-1R-NEO
wv-1
(bp)
7,743
F
W-1
W-1R-NEO
W-1R
WV-1
5′ external
3′ external
neo
−12118 bp
−8490 bp
−12118 bp
−6369 bp
−8490 bp
G
W mutation
W-1 ntESCs
W-1R ntESCs
Transposon-excised site
H
W-1 genital ridges
W-1R genital ridges
I
Vasa
SSEA1
Hoechst
Merge
W-1
W-1R

jection of these cells into the CD1 tetraploid blastocysts, we detected well-organized germ cells in E12.5 reconstructed embryos (Figure 2H). Fluorescence staining showed that E12.5 genital ridges originated from W-1R and WV-1 cells contained SSEA1 and Vasa double-positive primordial germ cells (PGCs), whereas only few positive PGCs appeared in the W-1-reconstructed fetus (Figure 2I and Supplementary information, Figure S2D). These results suggest that the *c-Kit* gene affects germ cell specification *in vivo*, which is consistent with previous reports [19], and that the germ cell mutant phenotype was rescued by gene correction. In summary, the repaired ntESCs could differentiate into germ cells *in vivo*.

Germ cell specification of repaired ntESCs in vitro

To investigate the germ cell specification of the repaired cells *in vitro*, we first differentiated the W-1, W-2, repaired ntESCs (W-1R and W-2R), and WV-1 ESCs into epiblast-like cells (EpiLCs) following the published protocol [21]. ESCs were cultured in feeder-free condition and passaged for at least three times before differentiation. The EpiLCs emerged after treating the cells with activin A and bFGF. Real-time PCR and immunostaining analyses showed that *Oct4* expression was maintained at a high level in EpiLCs, whereas the expression levels of *Nanog* and *Sox2* decreased. There was no significant difference in expression of these genes among the three groups (Figure 3A, 3B and Supplementary information, Figure S3A and S3B). Moreover, the expression of naive stem cell marker genes including *Prdm14*, *Zfp42*, *Tbx3*, *Tcl1*, *Esrrb*, *Klf2*, *Klf4* and *Klf5* was downregulated, while the expression of primed stem cell marker genes including *Fgf5*, *Wnt3a*, *Dnmt3b* and *Brachyury* (*T*) was significantly upregulated (Figure 3B and Supplementary information, Figure S3B). The endoderm markers (*Gata4*, *Gata6*, *Sox17* and *Blimp1*) remained at very low levels (Figure 3B and Supplementary information, Figure S3B). In short, there was no significant gene expression difference among the unrepaired ntESCs, repaired ntESCs and WV-1 ESCs.

We next examined whether all three groups of EpiLCs could be induced into PGCLCs under the previously described conditions with slight modifications. N2B27 medium supplemented with 15% KSR, BMP4/BMP8a, EGF, SCF and LIF was used for differentiation. After 6 days of PGCLC differentiation, about 10% integrin β3 and SSEA1 double-positive cells were detected in W-1R EpiLCs by FACS analysis, whereas few double-positive cells were detected in W-1 derivatives (Figure 3C). Real-time PCR results revealed that the expression levels of pluripotency genes including *Sox2* and *Nanog* were significantly increased in day-6 integrin β3 and SSEA1 double-positive cells (Figure 3D). The expression levels of PGC-related genes such as *Blimp1*, *Prdm14*, *Tcfap2c, Nanos3*, *Stella*, *Tdrd5*, *Dnd1* and *Dnmt1* were also increased in the late stage of differentiation, while the expression of Np95 and *Dnmt3a/3b* was downregulated (Figure 3D). In contrast, the derivatives of W-1 cells showed very low expression levels of numerous genes related to PGCLC specification compared with W-1R and WV-1 derivatives (Supplementary information, Figure S3C). Western blot analysis of W-1R derivatives showed reduced levels of H3K9me2 and increased levels of H3K27me3 from EpiLC to PGCLC differentiation (Figure 3E). Bisulfate sequencing of the DMRs (differentially methylated regions) of maternal imprinting genes *Igf2r* and *Snrpn*, and paternal imprinting genes *H19* and *Kcnq1ot1* showed that W-1R PGCLCs largely retained methylation of *H19* and *Kcnq1ot1*, and showed reduced methylation in *Igf2r* and *Snrpn*, indicating that erasure of imprints was initiated in W-1R PGCLCs (Figure 3F).

Collectively, in the EpiLC differentiation stage, there was no significant difference among all three groups. However, in the PGCLC differentiation stage, the PGCLCs from W-1R and WV-1 cells exhibited upregulated expression of germ cell-associated genes, but W-1 EpiLCs could not efficiently differentiate into PGCLCs (Figure 3D and Supplementary information, Figure S3C).

Figure 2 Correction of the *W* mutation of *c-Kit* gene in ntESCs (related to Supplementary information, Figure S2 and Tables S1 and S3). **(A)** Scheme for correction of the *c-Kit* gene *W* point mutation in W-1 ntESCs. **(B)** TALEN recognition sequence and FokI action site. **(C)** Sequences of wild-type (top line, Kit^{+}), *W* mutation (second line, Kit^{w}), piggyBac (third line, Kit^{PB}), and repaired (fourth line, Kit^{Rev}) alleles. Changes in the sequences of Kit^{Rev} allele introduced by the transposon excision are indicated with asterisks. **(D)** The strategy for precise genome modification using TALEN and piggyBac transposon. Top line, partial structure of the *c-Kit* gene; red arrow, PCR primers; black box, exons; double arrow, piggyBac transposon; blue line, probes for Southern blot analysis. **(E)** PCR analysis of the insertion. **(F)** Southern blot analysis of the 5′ homologous arm, 3′ homologous arm and NEO in W-1, W-1R-NEO, W-1R, and WV-1 cells. **(G)** DNA sequencing of the *c-Kit* gene *W* point mutation in the W-1 and W-1R cells. **(H)** The genital ridges and mesonephros of E12.5 tetraploid complementation fetus from W-1 and W-1R ntESCs. **(I)** Immunostaining of the genital ridges and mesonephros of E12.5 tetraploid complementation fetus from W-1 and W-1R ntESCs (Vasa (green) and SSEA1 (red)). Nuclei were stained with Hoechst 33342 (blue). Scale bar = 100 μm.

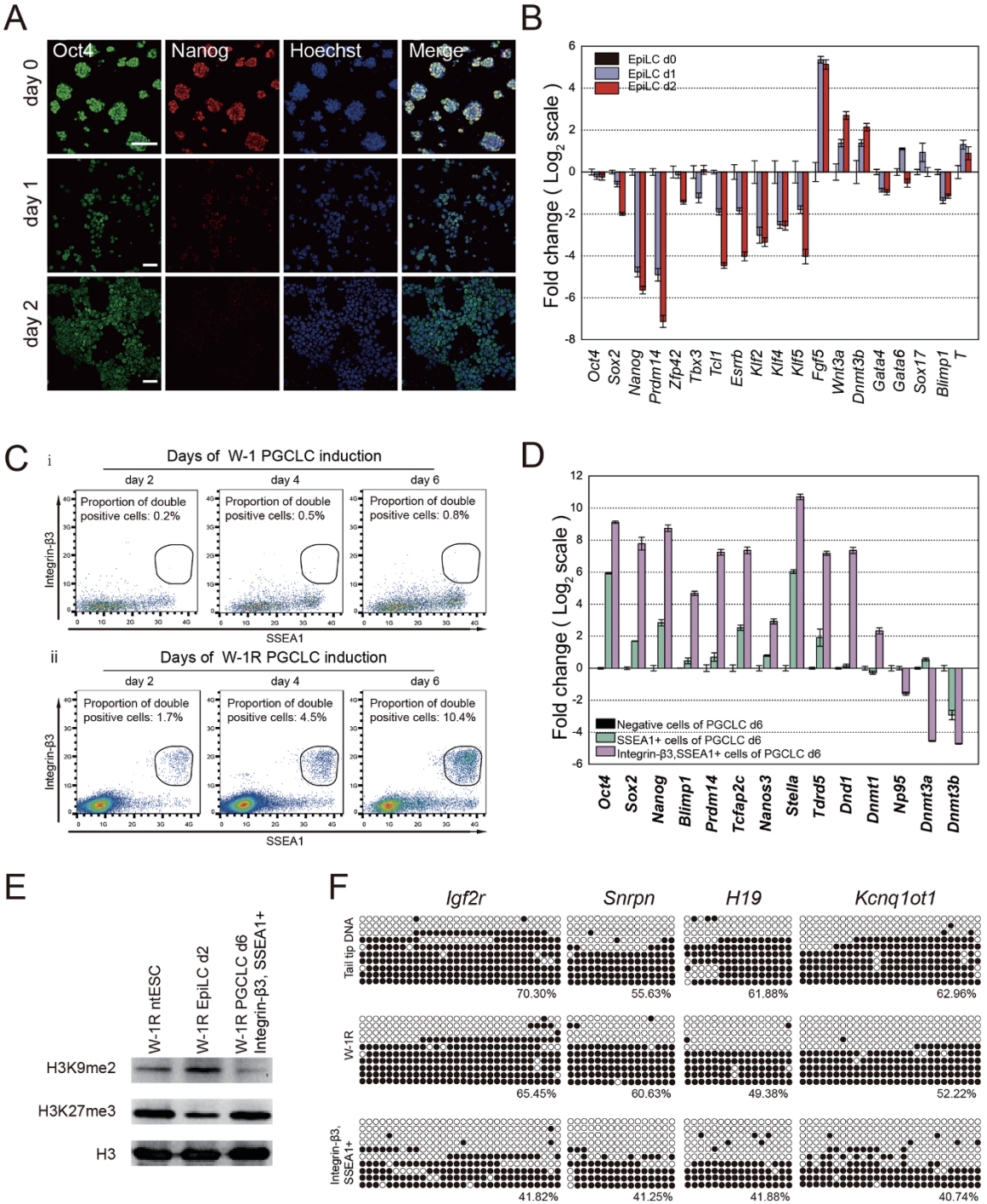

Figure 3 EpiLCs (from W-1R, P28) were differentiated into PGCLCs (related to Supplementary information, Figure S3 and Table S3). **(A)** Immunostaining of the W-1R EpiLCs (d0, d1, and d2) with anti-Oct4 (left) and anti-Nanog (middle). Nuclei were stained with Hoechst 33342 (blue; right). Scale bar = 50 μm. **(B)** Gene expression profiles during the EpiLC induction (triple repeats). The value for ntESCs (W-1R, P28) was set as 0. The average value is shown in the $\log_2$ scale. **(C)** FACS sorting of SSEA1 and integrin β3 double-positive cells on day 2, 4, and 6 aggregates differentiated from W-1 (upper) and W-1R (lower) cells. **(D)** Gene expression profiles of SSEA1 and integrin β3 double-positive cells on day 6 after PGCLC induction. The average value is plotted on the $\log_2$ scale with SDs. **(E)** Western blot analyses of H3K9me2 and H3K27me3 in W-1R ntESCs, W-1R d2 EpiLCs, and W-1R d6 PGCLCs (SSEA1 and integrin β3 double-positive cells). **(F)** Bisulfite sequencing of DMRs of *Igf2r*, *Snrpn*, *H19* and *Kcnq1ot1* in wild-type tail tip tissues, W-1R ntESCs and W-1R day-6 PGCLCs (SSEA1 and integrin β3 double-positive cells). White and black circles indicate unmethylated and methylated CpGs, respectively.

Together, these data suggest that the *c-Kit* gene may affect the specification or proliferation of the PGCLCs both *in vivo* and *in vitro*.

Generation of fertile transgenic offspring with gametes derived from RFP-PGCLCs

To facilitate the tracing of transplanted PGCLCs, we introduced a red fluorescent protein (RFP) cassette (Supplementary information, Figure S4A) into the repaired cell lines by electroporation and purified RFP-positive cells by FACS. Two RFP-positive cell lines (W-1R^{RFP}and W-2R^{RFP}) were obtained for PGCLC differentiation (Figure 4A and Supplementary information, Figure S4B). The SSEA1 and integrin β3 double-positive PGCLCs were transplanted into busulfan-treated testes based on the method described previously [22, 23]. The endogenous spermatogenesis of the recipient mice was severely impaired before transplantation (Supplementary information, Figure S4C). Two months after the transplantation, numerous RFP-positive cells were observed in the sem-

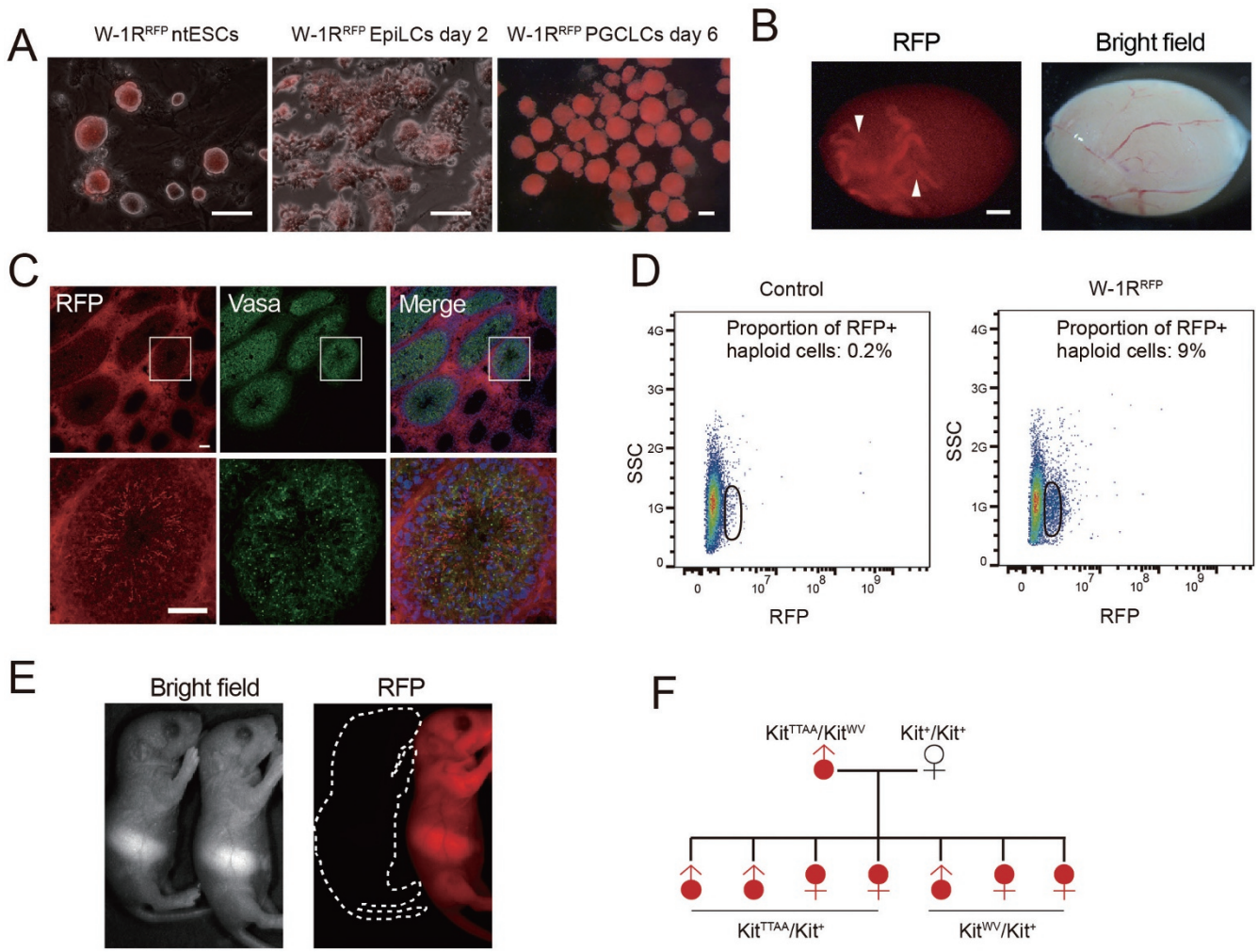

Figure 4 Spermatogenesis and production of healthy offspring from transplantation of W-1R^{RFP} PGCLCs (related to Supplementary information, Figure S4 and Tables S2 and S3). **(A)** Cell fluorescence detection of EpiLCs day 0, EpiLCs day 2 and PGCLC day 6 of piggyBac-RFP-labeled W-1R^{RFP} cells. Scale bar = 100 μm. **(B)** Testis of busulfan-treated mouse after transplantation of SSEA1/integrin β3 double-positive PGCLCs differentiated from W-1R^{RFP} cells. Arrow heads indicate RFP^{+} seminiferous tubules. Scale bar = 1 mm. **(C)** Immunostaining of the testes shown in **B** with anti-Vasa antibody (green). Hoechst 33342 (blue) stained the nuclear DNA. An RFP and Vasa double-positive region enclosed by a rectangle is enlarged and shown in the lower panel. Scale bar = 50 μm. **(D)** Percentage of RFP^{+} cells in the haploid cells isolated from seminiferous tubules determined by FACS analysis. **(E)** The offspring derived from the RFP-expressing spermatozoa. The wild-type newborn mouse (left) was the control. **(F)** A family tree of W-1R^{RFP} and W-2R^{RFP} offspring.

Table 1 Summary of transplantation of the PGCLCs into the busulfan-treated or Kit^{w}/Kit^{wv} mouse testes

Parental cells	Transferred cells	Recipient testes	No. of testes transplanted	No. of cells transplanted/testis	No. of testes with teratoma (%)	No. of testes with spermatogenesis (%)
W-1	Nonsorted cells	Busulfan-treated	10	1×10^4	5/10 (50)	Not determined
W-1R	Integrin-β3, SSEA1 (+) cells	Busulfan-treated	22	1×10^4	0/22	8/22 (36)
W-2R	Integrin-β3, SSEA1 (+) cells	Busulfan-treated	16	1×10^4	0/6	3/16 (18)
$W\text{-}1R^{RFP}$	Integrin-β3, SSEA1 (+) cells	Busulfan-treated	42	1×10^4	0/42	17/42 (40)
$W\text{-}2R^{RFP}$	Integrin-β3, SSEA1 (+) cells	Busulfan-treated	18	1×10^4	0/18	5/18 (28)
W-1R	Integrin-β3, SSEA1 (+) cells	Kit^{w}/Kit^{wv}	6	1×10^4	0/6	4/6 (66.7)

iniferous tubules with no obvious tumorigenesis (Figure 4B, Table 1 and Supplementary information, Figure S4E). Meanwhile, half recipient testes transplanted with nonsorted W-1 cells that have undergone *in vitro* PGCLC differentiation produced tumors (Table 1 and Supplementary information, Figure S4D). An immunostaining assay showed that these red fluorescent cells were well organized in the seminiferous tubules and expressed Vasa (Figure 4C) and AFAF (Supplementary information, Figure S4F), indicating that the transplanted cells have survived and located in the bottom of the seminiferous epithelium.

To further demonstrate the function of these sperm cells, the isolated RFP-positive seminiferous tubules were digested, and the haploid cells with RFP fluorescence were harvested by FACS selection and used for intracytoplasmic sperm injection (ICSI). The proportion of obtained RFP-positive haploid cells was about 9% (Figure 4D). After the ICSI, 83 embryos that developed to 2-cell stage were transplanted into the uterus of the pseudo-pregnant mice (Supplementary information, Table S2). Seven pups with RFP expression were obtained (Figure 4E, 4F and Supplementary information, Table S2). The results of DNA sequencing analysis showed that, among the seven pups, four carried the repaired allele, and the other three carried the *WV* mutation, consisting with the Mendelian law (Figure 4F and Supplementary information, Figure S4G). Together, these data showed that the repaired ntESCs could generate functional sperms after differentiation.

Generation of functional spermatids from PGCLC co-transplantation with EGFP-labeled testis somatic cells

We further explored the feasibility of generating functional sperms without genetic labeling for future clinical applications. After PGCLC differentiation of W-1R and W-2R cells, SSEA1 and integrin β3 double-positive PGCLCs were selected by FACS, and then were co-transplanted with EGFP-labeled testis somatic cells at the ratio of 1:3 into busulfan-treated mouse testes. $EGFP^{+}$ testis somatic cells were isolated from the testes of about 1-week-old mice (Figure 5A). Immunostaining of GATA4 (sertoli cell marker) and Vasa (germ cell marker) showed rare residence of germ cells in the $EGFP^{+}$ testis somatic cell population (Supplementary information, Figure S5A). Eight weeks after the cotransplantation, EGFP-positive seminiferous tubules (Figure 5B) were dissected and digested. The haploid cells were collected for ICSI. After injection, 71 embryos out of the 93 injected embryos developed to 2-cell stage, which were then transplanted into the uterus of the pseudo-pregnant mice (Supplementary information, Table S2). Nine pups were born, and genotyping analysis confirmed that two pups inherited the corrected allele from the repaired ntESCs (Figure 5C-5E). However, the other seven pups did not contain either the corrected or the WV allele. One possibility was that part of spermatids were derived from the spermatogenesis recovery of the busulfan recipient mice, not from PGCLCs. The two corrected pups could survive to adulthood and were fertile (Figure 5F). These data suggest that PGCLCs co-transplanted with labeled testis somatic cells could also undergo proper spermatogenesis. These EGFP-labeled testis somatic cells will facilitate further identification and isolation of the gametes.

The spermatogenesis potential was restored in Kit^{w}/Kit^{wv} infertile mouse after PGCLC transplantation

In order to check the spermatogenesis capacity of these PGCLCs in infertile mouse, we then transplanted the W-1R ntESC-derived PGCLCs into seminiferous tubules of Kit^{w}/Kit^{wv} neonatal mouse testis (Table 1). Eight weeks later, obvious spermatogenesis could be detected in four out of six recipient testes (Table 1); larger tubules could be found mixed with thinner ones without spermatogenesis within one testis (Figure 6A). The large tubules contained many spermatozoa which had normal morphology (Figure 6B). The H&E staining showed that the recipient testis had robust spermatogenesis (Figure 6C). Vasa and PNA double-positive germ cells appeared

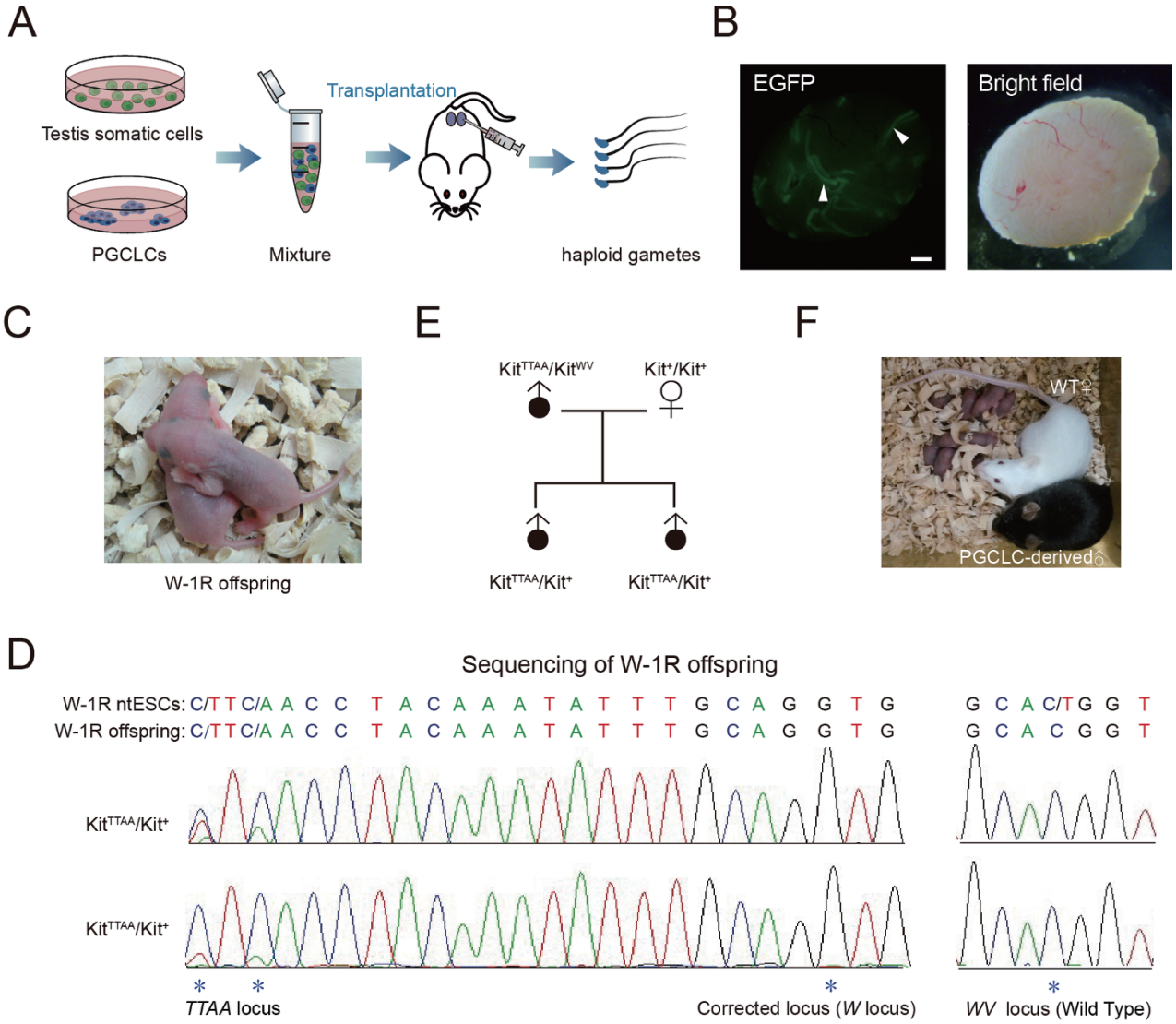

Figure 5 Generation of functional sperms from PGCLCs co-transplanted with EGFP$^+$ testis somatic cells (related to Supplementary information, Figure S5 and Tables S2 and S3). **(A)** Scheme for spermatogenesis of PGCLCs co-transplanted with EGFP$^+$ testis somatic cells. **(B)** Testis of busulfan-treated mouse after co-transplantation of SSEA1 and integrin β3 double-positive PGCLCs differentiated from W-1R cell line and EGFP$^+$ testis somatic cells. Arrow heads indicate EGFP-positive seminiferous tubules. Scale bar = 1 mm. **(C)** Two pups carrying the corrected allele were obtained via ICSI using W-1R spermatozoa. **(D)** DNA sequencing of the *W* and *WV* point mutations in the *Kit* gene in W-1R offspring. **(E)** A family tree of W-1R offspring. **(F)** Offspring of one mouse shown in **C** after mating with a wild-type female mouse.

in the large tubules (Figure 6D). To evaluate the function of the spermatozoa, ICSI was performed. Totally, 33 oocytes were injected, and 28 embryos developed to 2-cell stage. After transplantation into the uterus of the pseudo-pregnant mice, one healthy pup was obtained (Figure 6E and Supplementary information, Table S2). DNA sequencing analysis showed that it only carried the *WV* mutation (Figure 6F). All these results revealed that the repaired ntESC-derived PGCLCs had proper spermatogenesis in *Kit^W/Kit^{WV}* infertile mouse.

Discussion

In this study, we generated ntESCs from the fibroblasts of *Kit^W/Kit^{WV}* infertile adult male mice and corrected the gene mutation using the TALEN gene-editing system. By differentiation *in vitro*, the repaired ntESCs (W-1R, W-2R, W-1R^{RFP}, and W-2R^{RFP}) could generate functional PGCLCs, while the unrepaired ntESCs (W-1) failed to generate sufficient PGCLCs. The repaired ntESCs labeled with a RFP-expressing cassette could generate

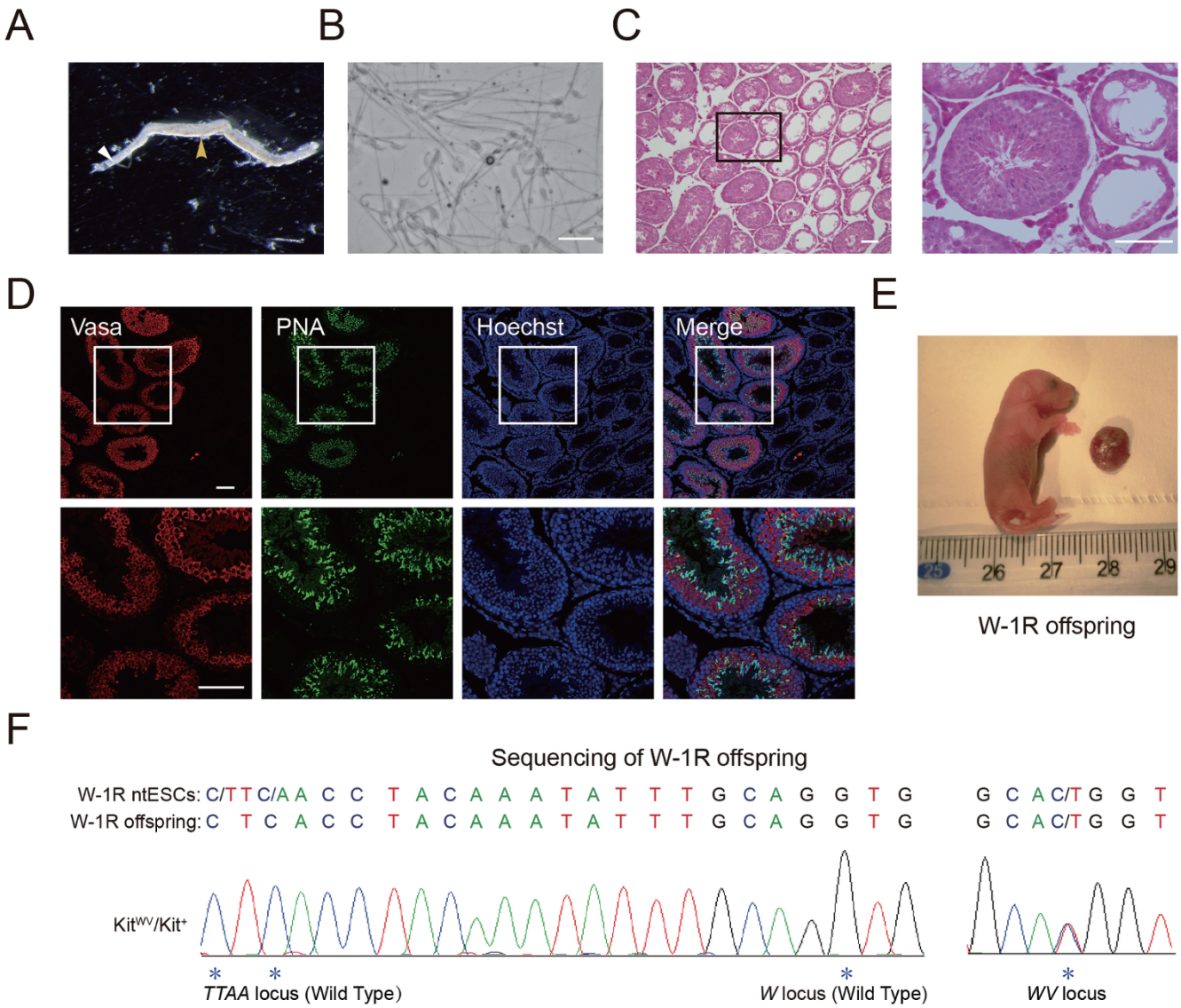

Figure 6 Spermatogenesis in *Kit*^{w}*/Kit*^{wv} mouse testis after PGCLC transplantation. **(A)** A single seminiferous tubule transplanted with the PGCLCs, showing (white arrow head) or not showing (yellow arrow head) spermatogenesis. **(B)** Spermatozoa derived from the PGCLCs. Scale bar = 20 μm. **(C)** Sections of the PGCLC-transplanted testes after H&E staining. Scale bar = 100 μm. **(D)** Immunostaining of the PGCLC-transplanted testes with anti-Vasa (red) and PNA (green). Hoechst 33342 (blue) stained the DNA. Scale bar = 100 μm. **(E)** One live offspring generated by ICSI using W-1R spermatozoa. **(F)** DNA sequencing of *W* and *WV* point mutations of the offspring shown in **E**.

functional sperms after being transplanted into busulfan-treated testes and give birth to offspring containing the RFP transgene. Via co-transplantation with EGFP-labeled testis somatic cells into busulfan-treated testes or transplantation into *Kit*^{w}*/Kit*^{wv} infertile testes, unlabeled PGCLCs could also generate functional spermatids.

Combination of reprogramming and cell therapy has been successfully applied to treat various genetic diseases in animal models [24]. However, the concern that iPSCs and their derivatives may transform to tumor cells may hinder the clinical application of iPSCs [25]. Recently, both human and mouse SCNT ESCs were reported to more closely resemble the relative ESCs [26, 27]. In addition, cells may also accumulate mutations at both genetic and epigenetic levels when subjected to gene correction and long-time *in vitro* culture. Here we corrected the ntESCs with the TALEN gene-editing system with no residual exogenous DNA. Our transplantation experiments proved that the transplanted differentiated cells did not induce tumor formation within 2 months. In addi-

tion, the birth of healthy offspring also indicated that the ntESCs have maintained the genomic integration during the whole *in vitro* culture. A recent study showed that the highly efficient CRISPR-Cas9 system can be used to correct the gene mutation in spermatogonial stem cells (SSCs) to rescue genetic diseases in mouse [28], which may have the potential application in treating people who can produce SSCs but contain genetic defects, while our approach may restore the fertility of people who lack germ cells. These results open the avenue for the treatment of male infertility and other genetic diseases in a safer way.

Genetic mutations are one of the causes of male infertility. Currently, there is no effective strategy for regeneration of functional gametes. Using the method of combining somatic reprogramming and gene correction, we may be able to generate repaired human PSCs. With the advance of maintaining the ground state of human naive stem cells equivalent to mouse ESCs [29], it is possible that the repaired human PSCs could further differentiate into functional haploid cells using a similar germ cell differentiation protocol in mouse. In addition, an infertile male patient may harbor multiple SNP mutations, of which phenotypes could be difficult to correct [30]. With the aid of genetic analysis, we can identify the critical mutations and correct them using gene editing tools like the TALEN or CRISPR/Cas system to rescue the male infertility. Taken together, our experiments in mouse model raise the possibility that infertile male patients with genetic mutations could be treated with the combination of reprogramming and gene-editing technologies.

Materials and Methods

Generation of the Kit^{w}/Kit^{wv} ntESCs

The methods to generate ntESCs were described previously [31]. Briefly, donor nuclei or chromosomes of TTFs from the Kit^{w}/Kit^{wv} mutant mice (Jackson Lab) were removed from donor cells and injected into recipient B6DF1 M II oocytes, and the meiotic metaphase plate was removed while withdrawing the pipette from cytoplasm after injection. Then the hybrids were activated and cultured until the blastocyst stage. The blastocysts were placed in a well of a 4-well plate pre-coated with mouse feeder cells [32]. For feeder-free culture, cells were maintained in a dish coated with poly-L-ornithine (0.01%; Sigma-Aldrich) and laminin (300 ng/ml; Invitrogen). The tetraploid complementation was performed as previously reported [33]. All cell lines have been tested for mycoplasma contamination. All animal experiments were performed in compliance with the guidelines of the Institute of Zoology, Chinese Academy of Sciences.

Correction of the W mutation in Kit^{w}/Kit^{wv} ntESCs

A TALEN pair was designed using the TALE-NT software. To improve the expression of the TALEN pair in mammalian cells, N- and C-terminal elements of TALE plus the FokI domain from pTAL3 were inserted into pCDNA3.1 (−) by *Bgl*II/*Bam*HI and *Afl*II. Repeat-variable diresidues were assembled using Golden Gate kit as described [34]. To construct the donor vector, the homologous arm (HA) was amplified by using the mouse genomic DNA as a template. Four kb right HA was inserted into pL253 by *Not*I and *Xba*I, followed by insertion of 1 kb left HA by *Not*I and *Hpa*I. To construct the piggyBac-NEO vector, the NEO cassette cut from pL452 by *Xho*I was inserted into the PB-CAG-rtTA vector [35], which was then digested by *Sal*I to remove CAG-rtTA. The PB 3′ and 5′ TR-NEO cassette was PCR amplified from the piggyBac-NEO vector and inserted into the pL253-HA by *Hpa*I. Donor vector was confirmed by sequencing. Primers used are listed in Supplementary information, Table S3.

The TALEN plasmids and the donor vector were transfected into the cell line. G418 and GANC selection were performed, and drug-resistant clones were picked and screened by PCR. To remove the piggyBac-flanked selection cassette from these modified clones, a hyperactive form of the piggyBac transponsase was transiently transfected into the corrected clones, which were then subjected to sequencing of the *W* locus.

Southern blot

Genomic DNA (20 g) was digested by *Eco*RV (Takara, Dalian, China) for each probe and recovered by alcohol precipitation. Digested genomic DNA was separated on a 0.8% agarose gel and transferred to a nylon membrane (GE Healthcare). DIG High Prime DNA Labeling and Detection Starter Kit I (Roche) was used to perform probe labeling, hybridization and immunological detection according to the manufacturer's instructions. Primers used for amplifying probes were listed in Supplementary information, Table S3.

Induction of EpiLCs and PGCLCs

The methods to induce EpiLCs and PGCLCs from ntESCs were described previously [21]. Briefly, the EpiLCs were induced by plating 1×10^5 ESCs in a well of a 12-well plate coated with human plasma fibronectin in N2B27 medium containing activin A, bFGF, and KSR. The PGCLCs were induced under a floating condition by plating 2×10^3 EpiLCs in a well of a low-cell-binding U-bottom 96-well plate in a special medium (N2B27 with 15% KSR, BMP4, LIF, SCF, BMP8b, and EGF).

Immunohistochemistry

The testes of PGCLC-transplanted mice were excised, fixed in 4% paraformaldehyde (PFA) in PBS at room temperature overnight and embedded in OCT. Cryosections (20-μm thick) were blocked with 0.3% Triton-X 100/2% BSA in PBS for 30 min before adding primary antibodies. For staining, the cells were fixed for 15 min with 4% PFA at room temperature. Primary antibodies used in this study are as follows: Oct4 (Santa Cruz Biotechnology), Nanog (Millipore), SSEA1 (Millipore), Vasa (Abcam), AFAF (Abcam), *DAZL* (Abcam), and Gata4 (Abcam). All samples were washed three times in PBS after incubating at 4 °C overnight, and then incubated with secondary antibodies for 1 h. The secondary antibodies were FITC, Cy3, or Cy5 labeled (Jackson Immuno Research). The DNA was counterstained with 10 μg/ml Hoechst 33342 for 15 min and washed three times with PBS. Imaging was performed with the Zeiss LSM780 Meta inverted confocal microscope.

DNA and RNA isolation and real-time PCR

RNA was extracted with RNeasy Micro/Mini Kit (Qiagen) and reverse-transcribed using QuantiTect Reverse Transcription Kit (Qiagen). Real-time PCR was performed with gene-specific primers (Supplementary information, Table 3). At least three independent differentiation cultures were analyzed. DNA was extracted from tail tips of the mice or cell pellets in culture and genotyped as described [33]. PCR fragments of the *c-Kit* gene encompassing the *W* point mutation were amplified using the genomic DNA.

Flow cytometry analysis

PGCLCs were dissociated in 0.25% trypsin/1mM EDTA, re-suspended in PBS supplemented with 1% BSA, and then filtered through a 40-μm nylon mesh. The cells were incubated with SSEA1:AF647-conjugated mouse monoclonal IgM (eBioscience), integrin β3:FITC-conjugated mouse monoclonal IgG1 (BioLegend) for 30 min at 37 °C followed by FACS analysis. In order to obtain RFP^+ haploid cells, seminiferous tubules with a red fluorescence were separated using fine tweezers, and then dissociated in 0.25% trypsin/1mM EDTA for 10 min. After being filtered through a 40-μm nylon mesh, cell suspension was incubated in 10 μg/ml Hoechst 33342 for 20 min and prepared for FACS analysis. FACS analysis was performed using MoFlo XDP system (Beckman-Coulter).

Bisulfite sequencing

To confirm the DNA methylation state, sodium bisulfite treatment of DNA was performed by using EZ DNA Methylation-direct kit (Zymo Research). PCR amplification was performed using TAKARA HS DNA polymerase (Takara) with specific primers for *H19*, *Snprn*, *Igf2r*, and *Kcnq1ot1* DMRs. Primers used in this study are summarized in Supplementary information, Table S3. To determine the methylation state of individual CpG sites, the PCR product was extracted from the agarose gel, subcloned into pMD18T vector (Takara), and then sequenced. Methylation was analyzed by the web-based tool, QUMA (http://quma.cdb.riken.jp/), for visualization and quantification of the bisulfite sequencing data.

Transplantation of the PGCLCs

PGCLCs induced on day 6 were dissociated to single cells. Recipient animals (6-12-day-old male mice which were treated with busulfan at E12.5 in mother uterus or Kit^w/Kit^{wv} mutant male mice) were induced into hypothermic anesthesia on ice. The donor cell suspension (the FACS-sorted cells or together with sertoli cells from EGFP-transgenic mice) was injected into each testis [36]. The spermatozoa derived from the PGCLCs were isolated from the seminiferous tubules with RFP or EGFP expression two months after transplantation. The RFP^+ haploid cells (sorted by FACS) or all haploid cells derived from W-1R and W-2R cells were kept at 4 °C until ICSI.

Histological analysis

The removed testes were fixed in 4% PFA solution and embedded in paraffin. A series of sections (5 μm in thickness) were subjected to deparaffinization and dehydration, and then appropriate staining was performed. The tubule diameter was measured under light microscope.

ICSI and embryo transfer

ICSI was performed as described previously [37]. Briefly, the haploid round sperm cell suspension was added into 1 ml M2 medium supplemented with 5 μg/ml of cytochalasin B. Meanwhile, 15-20 pre-activated mature oocytes were placed in the M2 medium for 5 min. One haploid cell was injected into each single oocyte with Piezo driven pipette, and then the ICSI embryos were transferred into the activation medium and incubated for 5 h. Two-cell embryos were transferred into the oviduct of CD1 pseudo-pregnant females or further cultured to blastocyst stage *in vitro*. Full-term pups were obtained through natural labor or caesarean section.

Acknowledgments

We thank Dr Mitinori Saitou (Kyoto University, Japan) for help with germ cell differentiation and kindly providing BVSC mice and Dr Chunsheng Han (Institute of Zoology, Chinese Academy of Sciences) for help with germ cell transplantation. This work was supported by the National Basic Research Programs of China (2011CB944300 and 2012CB966500) and the National Natural Science Foundation of China (31322036 (Outstanding Young Scholars) and 31371506).

References

1 Hirsh A. Male subfertility. *BMJ* 2003; **327**:669-672.
2 Ferlin A, Raicu F, Gatta V, Zuccarello D, Palka G, Foresta C. Male infertility: role of genetic background. *Reprod Biomed* 2007; **14**:734-745.
3 O'Flynn O'Brien KL, Varghese AC, Agarwal A. The genetic causes of male factor infertility: a review. *Fertil Steril* 2010; **93**:1-12.
4 Tung JY, Rosen MP, Nelson LM, *et al.* Novel missense mutations of the Deleted-in-AZoospermia-Like (DAZL) gene in infertile women and men. *Reprod Biol Endocrinol* 2006; **4**:40.
5 Mosaad YM, Shahin D, Elkholy AA, Mosbah A, Badawy W. CAG repeat length in androgen receptor gene and male infertility in Egyptian patients. *Andrologia* 2012; **44**:26-33.
6 Soini S, Ibarreta D, Anastasiadou V, *et al.* The interface between assisted reproductive technologies and genetics: technical, social, ethical and legal issues. *Eur J Hum Genet* 2006; **14**:588-645.
7 Page DC, Silber S, Brown LG. Men with infertility caused by AZFc deletion can produce sons by intracytoplasmic sperm injection, but are likely to transmit the deletion and infertility. *Hum Reprod* 1999; **14**:1722-1726.
8 Nocka K, Tan JC, Chiu E, *et al.* Molecular bases of dominant negative and loss of function mutations at the murine c-kit/white spotting locus: W37, Wv, W41 and W. *EMBO J* 1990; **9**:1805-1813.
9 Huang E, Nocka K, Beier DR, *et al*. The hematopoietic growth factor KL is encoded by the Sl locus and is the ligand of the c-kit receptor, the gene product of the W locus. *Cell* 1990; **63**:225-233.
10 Chabot B, Stephenson DA, Chapman VM, Besmer P, Bernstein A. The proto-oncogene c-kit encoding a transmembrane tyrosine kinase receptor maps to the mouse W locus. *Nature* 1988; **335**:88-89.
11 Yamanaka S, Blau HM. Nuclear reprogramming to a pluripo-

tent state by three approaches. *Nature* 2010; **465**:704-712.
12 Tachibana M, Amato P, Sparman M, *et al.* Human embryonic stem cells derived by somatic cell nuclear transfer. *Cell* 2013; **153**:1228-1238.
13 Wakayama T, Tabar V, Rodriguez I, Perry AC, Studer L, Mombaerts P. Differentiation of embryonic stem cell lines generated from adult somatic cells by nuclear transfer. *Science* 2001; **292**:740-743.
14 Takahashi K, Yamanaka S. Induction of pluripotent stem cells from mouse embryonic and adult fibroblast cultures by defined factors. *Cell* 2006; **126**:663-676.
15 Takahashi K, Tanabe K, Ohnuki M, *et al.* Induction of pluripotent stem cells from adult human fibroblasts by defined factors. *Cell* 2007; **131**:861-872.
16 Wu Y, Liang D, Wang Y, *et al.* Correction of a genetic disease in mouse via use of CRISPR-Cas9. *Cell Stem Cell* 2013; **13**:659-662.
17 Reinhardt P, Schmid B, Burbulla LF, *et al.* Genetic correction of a LRRK2 mutation in human iPSCs links parkinsonian neurodegeneration to ERK-dependent changes in gene expression. *Cell Stem Cell* 2013; **12**:354-367.
18 Xu J, Peng C, Sankaran VG, *et al.* Correction of sickle cell disease in adult mice by interference with fetal hemoglobin silencing. *Science* 2011; **334**:993-996.
19 Runyan C, Schaible K, Molyneaux K, Wang Z, Levin L, Wylie C. Steel factor controls midline cell death of primordial germ cells and is essential for their normal proliferation and migration. *Development* 2006; **133**:4861-4869.
20 Zhang L, Tang J, Haines CJ, *et al.* c-kit and its related genes in spermatogonial differentiation. *Spermatogenesis* 2011; **1**:186-194.
21 Hayashi K, Ohta H, Kurimoto K, Aramaki S, Saitou M. Reconstitution of the mouse germ cell specification pathway in culture by pluripotent stem cells. *Cell* 2011; **146**:519-532.
22 Brinster CJ, Ryu BY, Avarbock MR, Karagenc L, Brinster RL, Orwig KE. Restoration of fertility by germ cell transplantation requires effective recipient preparation. *Biol Reprod* 2003; **69**:412-420.
23 Hermann BP, Sukhwani M, Winkler F, *et al.* Spermatogonial stem cell transplantation into rhesus testes regenerates spermatogenesis producing functional sperm. *Cell Stem Cell* 2012; **11**:715-726.
24 Gonzalez-Cordero A, West EL, Pearson RA, *et al.* Photoreceptor precursors derived from three-dimensional embryonic stem cell cultures integrate and mature within adult degenerate retina. *Nat Biotechnol* 2013; **31**:741-747.
25 Okita K, Ichisaka T, Yamanaka S. Generation of germline-competent induced pluripotent stem cells. *Nature* 2007; **448**:313-317.
26 Ma H, Morey R, O'Neil RC, *et al.* Abnormalities in human pluripotent cells due to reprogramming mechanisms. *Nature* 2014; **511**:177-183.
27 Li Z, Lu H, Yang W, *et al.* Mouse SCNT ESCs have lower somatic mutation load than syngeneic iPSCs. *Stem Cell Reports* 2014; **2**:399-405.
28 Wu Y, Zhou H, Fan X, *et al.* Correction of a genetic disease by CRISPR-Cas9-mediated gene editing in mouse spermatogonial stem cells. *Cell Res* 2015; **25**:67-79.
29 Gafni O, Weinberger L, Mansour AA, *et al.* Derivation of novel human ground state naive pluripotent stem cells. *Nature* 2013; **504**:282-286.
30 Hu Z, Xia Y, Guo X, *et al.* A genome-wide association study in Chinese men identifies three risk loci for non-obstructive azoospermia. *Nat Genet* 2011; **44**:183-186.
31 Zhao C, Yao R, Hao J, *et al.* Establishment of customized mouse stem cell lines by sequential nuclear transfer. *Cell Res* 2007; **17**:80-87.
32 Ying QL, Wray J, Nichols J, *et al.* The ground state of embryonic stem cell self-renewal. *Nature* 2008; **453**:519-523.
33 Zhao XY, Li W, Lv Z, *et al.* iPS cells produce viable mice through tetraploid complementation. *Nature* 2009; **461**:86-90.
34 Cermak T, Doyle EL, Christian M, *et al.* Efficient design and assembly of custom TALEN and other TAL effector-based constructs for DNA targeting. *Nucleic Acids Res* 2011; **39**:e82.
35 Wang W, Yang J, Liu H, *et al.* Rapid and efficient reprogramming of somatic cells to induced pluripotent stem cells by retinoic acid receptor gamma and liver receptor homolog 1. *Proc Natl Acad Sci USA* 2011; **108**:18283-18288.
36 Chuma S, Kanatsu-Shinohara M, Inoue K, *et al.* Spermatogenesis from epiblast and primordial germ cells following transplantation into postnatal mouse testis. *Development* 2005; **132**:117-122.
37 Li W, Shuai L, Wan H, *et al.* Androgenetic haploid embryonic stem cells produce live transgenic mice. *Nature* 2012; **490**:407-411.

(**Supplementary information** is linked to the online version of the paper on the *Cell Research* website.)